Hindawi
Mathematical Problems in Engineering
Volume 2021, Article ID 8834547, 13 pages
https://doi.org/10.1155/2021/8834547

Research Article

Simulation Research on Trapped Oil Pressure of Involute Internal Gear Pump

Shanxin Guo [1] **and Xiangfeng Guan** [2]

[1]*College of Electronics and Information Science, Fujian Jiangxia University, Fuzhou 350108, China*
[2]*Smart Home Information Collection and Processing on Internet of Things Laboratory of Digital Fujian, Fuzhou 350108, China*

Correspondence should be addressed to Xiangfeng Guan; xfguan@fjjxu.edu.cn

Received 27 September 2020; Revised 27 December 2020; Accepted 7 January 2021; Published 18 January 2021

Academic Editor: A. M. Bastos Pereira

The main structure of an internal gear pump consisted of an internal gear pair, including an internal gear and an external gear. The internal gear pump had oil trapping phenomenon like other hydraulic gear pumps. In order to solve the oil trapping phenomenon of involute gear pump with internal meshing tooth profile, in this paper, the mathematical equation of gear outer contour is established according to the principle of generation method, and the variation law of the trapped oil area in meshing process is deduced by theoretical instantaneous flow rate obtained by scanning method. Then, the minimum trapped oil volume and unloading area are solved by the graphic method. Finally, based on fluid mechanics and dynamics, the trapped oil pressure model is obtained. The change of the trapped oil area and trapped oil pressure in a meshing cycle is simulated by MATLAB. The results show that the trapped oil area changes in a parabola, and the trapped pressure fluctuates in mountains and valleys. When the trapped area is the smallest, the trapped oil pressure reaches the peak at the corresponding corner. The research results can provide guidance for the development of high-performance internal gear pumps.

1. Introduction

In order to ensure the continuous and uniform oil supply of the gear pump, two pairs of gear teeth engaging in meshing are needed in the internal gear pump for a certain period of time. It results in a closed dead volume which is not connected with the inlet and outlet cavities [1]. The size of the closed dead volume changes periodically with the rotation of the gear, resulting in a dramatic change of the working pressure [2]. This phenomenon is usually called the oil trapping phenomenon of a gear pump, which is the main source of gear pump noise and cavitation [3]. It can cause hazards such as pressure swing, pressure shock, and flow pulsation in the hydraulic system [4]. Therefore, it is of great significance to avoid the so-called oil trapping phenomenon of the gear pump. However, because the trapped oil area is surrounded by complex curves such as the outer contour of gear, involute, or cycloid [5], it is very difficult to obtain the continuous and uniform oil supply. Up to date, there is much research on the oil trapping phenomenon of the external gear pump and cycloid gear [6], and great improvements have been made. In comparison with external gear pump and cycloid gear, internal gear pumps have advantages such as lighter weight, smaller volume, and higher pressure due to their geometric structure [7]. Because the internal gear has oil ports in the diameter direction and the oil trapping process is different from other gear pumps, the high-pressure internal gears are not easy to obtain by conventional fabrication methods of internal gears. The common internal meshing gears are arc tooth profile, conjugate tooth profile, involute tooth profile, and so forth. Most research is focused on arc tooth profile and conjugate tooth profile and there are a few studies on involute tooth profile [8]. In this study, in order to solve the oil trapping phenomenon of gear pump with involute tooth profile during the process of internal meshing, the contour of internal gear is obtained by means of an imaginary rack cutter generating internal gear, and the model of trapped oil

volume is established. Then, the design parameters and the change of trapped oil volume in the process of gear rotation are described, and then the trapped oil pressure is simulated. The research conclusion can provide an effective reference for the design and manufacture of the high-performance internal gear pump.

2. Mathematical Model

2.1. Oil Trapped Model of Internal Gear Pump. Gear pairs are commonly manufactured by the generative method [9]. Figure 1(a) shows the processing of external gears by the rack tool generating method, and Figure 1(b) shows the processing of the internal gears by the virtual rack tool generating method. The outer contour of the rack cutter is composed of line segments AB, CD, DE, and arc BC. The parameters of h_a, c_n, h_f, and r_0 are the addendum height, head clearance coefficient, total tooth height, and tool fillet, respectively. The parameters α, x, and p are pressure angle, the profile shift coefficient, and pitch, respectively. A rectangular coordinate system $s_t(O_t x_t y_t)$ is established at the center of the rack tool, and the mathematical equation of the rack tool is described as [10]

$$R_t^c(x_t) = \begin{bmatrix} R_t^{AB} & R_t^{BC} & R_t^{CD} & R_t^{DE} \end{bmatrix} = \begin{bmatrix} x_t^c \\ y_t^c \\ 1 \end{bmatrix}. \tag{1}$$

The coordinate systems of gears O_s and $O_{s'}$ are $s_s(O_s x_s y_s)$ and $s_{s'}(O_{s'} x_{s'} y_{s'})$, respectively. Their origins coincide with the gear axis and rotate with the gear axis. At the same time, the coordinate system $s_e(O_e x_e y_e)$ fixedly connected with the earth is established. During the forming process, the rack tool translates in the x_t direction, and the displacement is s. At this moment, the gear O_s rotates around O_e and the rotation angle is φ_s, which satisfies the following motion relationship:

$$s = r_s \varphi_s. \tag{2}$$

In the above equation, r_s is the gear pitch radius [11]:

$$r_s = 0.5mz, \tag{3}$$

where m and z are the modulus of the gear and the number of teeth, respectively.

According to the generation principle, the relationship between the tooth profile of the gear and the tooth profile of the rack tool can be expressed by the following equation [12]:

$$R_s^p(\varphi_s, x_t) = M_{st}(\varphi_s) R_t^c(x_t), \tag{4}$$

where the vector $R_s^p(\varphi_s, x_t)$ is the envelope of the tooth profile surface family of the rack tool and the matrix $M_{st}(\varphi_s)$ is the transformation matrix from the coordinate system s_s to the coordinate system s_t.

In the same way, the internal gear contour equation is obtained by the method of generating internal gears by imaginary rack tools:

$$R_t^p(\varphi_{s'}, x_t) = M_{s't}(\varphi_{s'}) R_t^c(x_t). \tag{5}$$

In the formula, the vector $R_t^p(\varphi_{s'}, x_t)$ is the envelope of the rack tool tooth profile surface family, and the matrix $M_{s't}(\varphi_{s'})$ is the transformation matrix from the coordinate system $s_{s'}$ to the coordinate system s_t.

2.2. Calculation of Trapped Oil Volume. The principle of the internal gear pump trapping oil is shown in Figure 2. The theoretical instantaneous flow Q_{sh} of the internal gear pump can be expressed as [13], which is derived [14] as

$$Q_{sh} = B\omega\left(r_a^2 - r^2 - r_j^2\varphi^2\right). \tag{6}$$

In equation (6), B is the gear face width, ω is the angular velocity of the gear pump; r_a is the addendum circle radius; r is the gear reference radius; r_j is the gear base circle radius, and φ is the driving gear rotation angle.

The scanning volume V_{sh} changes with the change of the driving gear rotation angle $\varphi$and the rate of change is [15]

$$\frac{dV_{sh}}{d\varphi} = \frac{Q_{sh}}{\omega} = B\left(r_a^2 - r^2 - r_j^2\varphi^2\right). \tag{7}$$

Figure 3 shows the relationship between the meshing point and the angle of rotation. The rotation angles corresponding to F, G, G', and F' are φ_F, φ_G, $\varphi_{G'}$, and $\varphi_{F'}$, respectively. The length between G and G' is h_j. The relationship between the rotation angles is$\varphi_G = (\pi/z) - \varphi_F$, $\varphi_{G'} = (1 + (2h_j/t_j))(\pi/z) - \varphi_F$, and $\varphi_{F'} = (2\pi/z) - \varphi_F$. The parameter of t_j is the base pitch.

The corresponding scan volume change rate is described as follows:

$$\frac{dV_F}{d\varphi_F} = B\left(r_a^2 - r^2 - r_j^2\varphi_F^2\right), \tag{8}$$

$$\frac{dV_G}{d\varphi_G} = B\left(r_a^2 - r^2 - r_j^2\varphi_G^2\right), \tag{9}$$

$$\frac{dV_{G'}}{d\varphi_{G'}} = B\left(r_a^2 - r^2 - r_j^2\varphi_{G'}^2\right), \tag{10}$$

$$\frac{dV_{F'}}{d\varphi_{F'}} = B\left(r_a^2 - r^2 - r_j^2\varphi_{F'}^2\right). \tag{11}$$

The change of trapped oil volume V, V_1, and V_2 with driving gear rotation angle φ is obtained by equations (8)–(11):

$$\frac{dV}{d\varphi} = \frac{4\pi}{z} B r_j^2 \left(\varphi - \frac{\pi}{z}\right), \tag{12}$$

$$\frac{dV_1}{d\varphi} = \frac{2\pi}{z}\left(1 - \frac{2h_j}{t_j}\right) B r_j^2 \left[\varphi - \frac{\pi}{2z}\left(1 - \frac{2h_j}{t_j}\right)\right], \tag{13}$$

$$\frac{dV_2}{d\varphi} = \frac{2\pi}{z} B r_j^2 \left(\varphi - \frac{3\pi}{2z}\right). \tag{14}$$

Integrating equations (12)–(14),

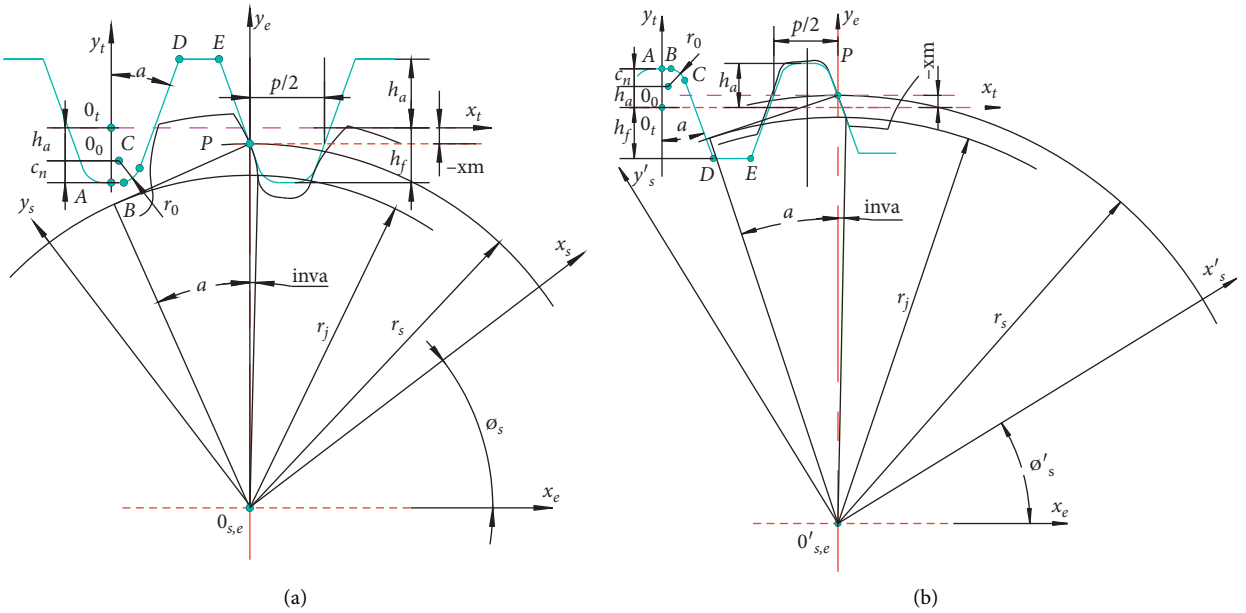

Figure 1: (a) Process external gears by generating method. (b) Virtual rack tool, internal gear processing by the generative method.

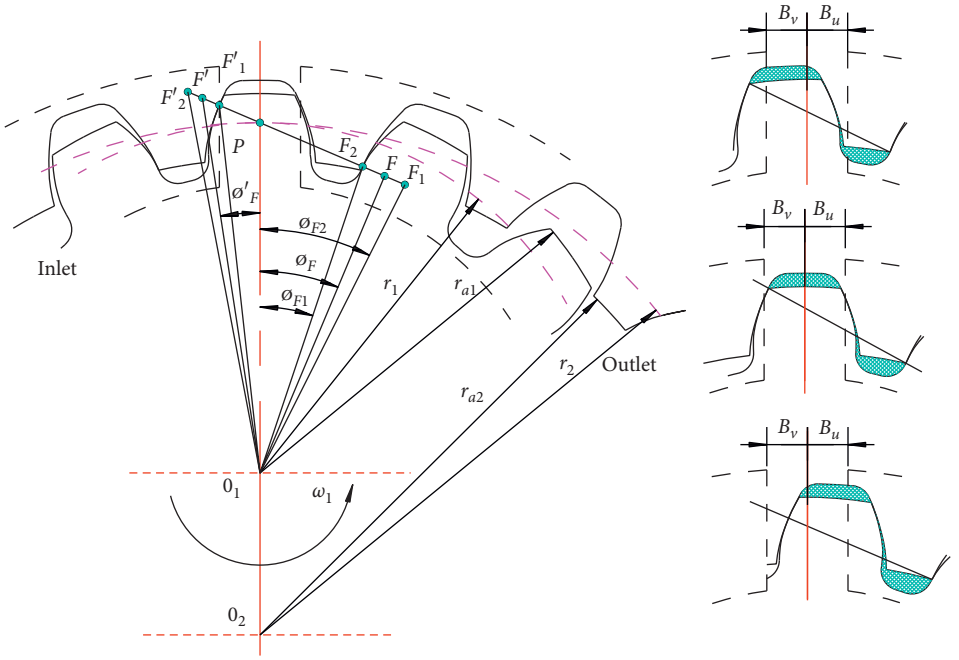

Figure 2: Oil trapping principle of the internal gear pump.

$$V = V_0 + \frac{2\pi}{z} B r_j^2 \left(\varphi - \frac{\pi}{z}\right)^2, \tag{15}$$

$$V_1 = V_{10} + \frac{\pi}{z}\left(1 - \frac{2h_j}{t_j}\right) B r_j^2 \left[\varphi - \frac{\pi}{2z}\left(1 - \frac{2h_j}{t_j}\right)\right]^2, \tag{16}$$

$$V_2 = V_{20} + \frac{\pi}{z} B r_j^2 \left(\varphi - \frac{3\pi}{2z}\right)^2. \tag{17}$$

From equations (15)–(17), V, V_1, and V_2 are the quadratic functions of the rotation angle φ. When $\varphi = (\pi/z)$, $(\pi/2z)(1 - (2h_j/t_j))$, $(3\pi/z)$, the minimum values V_0, V_{10}, and V_{20} are obtained, respectively.

2.3. Graphical Method to Solve the Minimum Trapped Oil Volumes $\mathbf{V_0}$, $\mathbf{V_{10}}$, $\mathbf{V_{20}}$. According to the definition of the trapped oil [5] and Figure 3, let $V_{\widehat{o1F'F}}$, $V_{\widehat{o2F'F}}$, $V_{\widehat{o1G'F3}}$, and

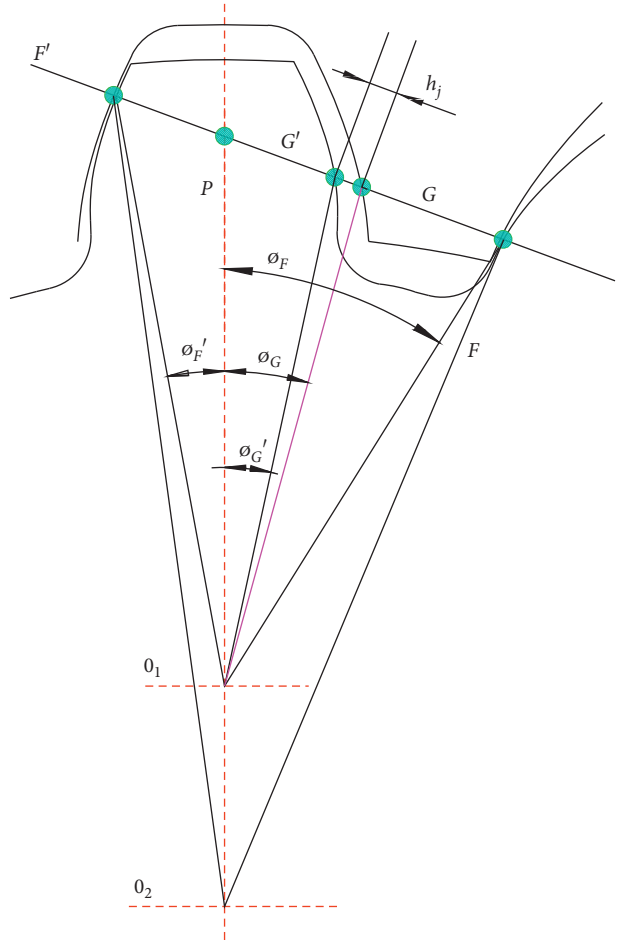

Figure 3: The relationship between the meshing point and the angle of rotation.

$V_{\overset{\frown}{o2GF3}}$ be the center of circle O_1, O_2 sector area, respectively. Let $V_{\Delta o1o2F}$ and $V_{\Delta o1o2F'}$ be the triangle area enclosed by O_1, O_2, F, F', G, and G', respectively. Then, the trapped oil volume can be described as

$$\begin{aligned} V &= V_{\overset{\frown}{o2F'F}} - V_{\overset{\frown}{o1F'F}} - \left(V_{\Delta o1o2F} + V_{\Delta o1o2F'}\right) = V_{\overset{\frown}{o2F'F}} - V_{\overset{\frown}{o1F'F}} - 0.5et_j\cos\alpha', \\ V_1 &= V_{\Delta o1G'F3} - V_{\overset{\frown}{o1G'F3}} + \left(V_{\Delta o2GF3} - V_{\overset{\frown}{o2GF3}}\right), \\ V_2 &= V - V_1. \end{aligned} \tag{18}$$

In the equation, e and α' are the distance between the center of the gear and the meshing angle of the gear pair.

In Figures 4 and 5, as the driving gear angle φ changes, $V_{\overset{\frown}{o2F'F}}$ and $V_{\overset{\frown}{o1F'F}}$ are composed of two parts: the unchanged area V_A and the changing area V_B. Then, the trapped oil volume V can also be expressed as

$$V = V_A + V_B - 0.5et_j\cos\alpha'. \tag{19}$$

In the equation, V_A consists of four sectors of area. The radius of the sector are the addendum circle $r_{a,1}$, $r_{a,2}$ and the tooth root circle $r_{f,1}$, $r_{f,2}$. The corresponding included angles of the sector are β_{11}, β_{21} enclosed:

$$V_A = 0.5r_{a,2}^2\beta_{21} + 0.5r_{f,2}^2\beta_{22} - 0.5r_{a,1}^2\beta_{12} - 0.5r_{f,1}^2\beta_{11}. \tag{20}$$

The derivation of area V_B is shown in Figure 6. The volume $V_{B\theta}$ occupied by the spread angle θ can be obtained by the following equation [16]:

$$V_{B\theta} = 0.5B\int r_k^2 d\theta + C. \tag{21}$$

In the equation, the pressure angle corresponding to the r_k radius on the tooth profile is θ.

Solve equation (21) definite integral:

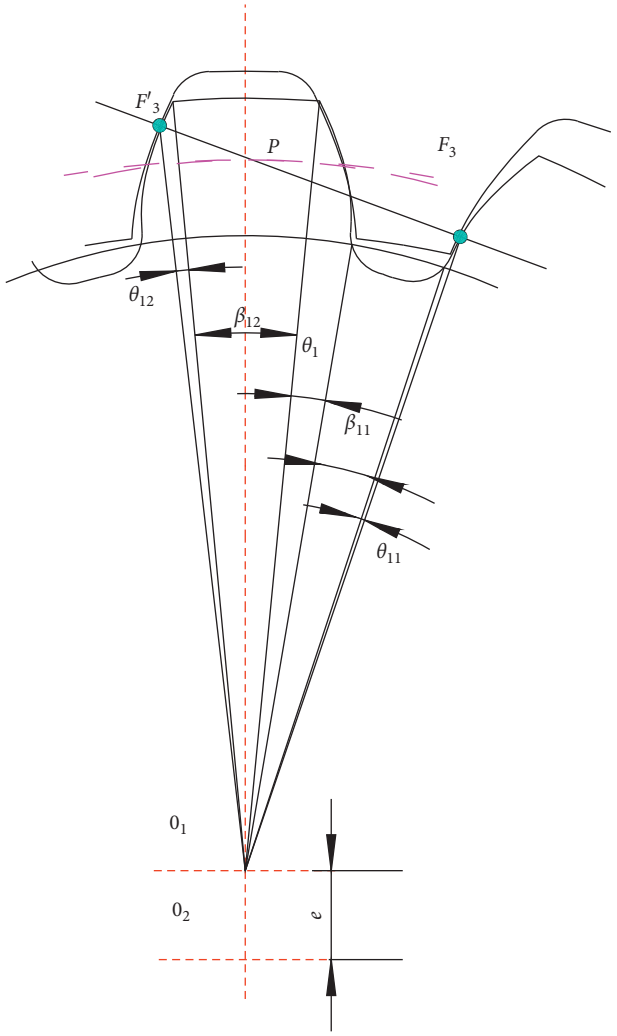

Figure 4: The relationship between the trapped oil and the rotation angle of the external gear.

$$V_\theta = \frac{Br_j^3}{6} r_a^3. \tag{22}$$

According to the principle of involute [17],

$$r = \theta + \alpha = \tan\alpha. \tag{23}$$

Therefore, when $r = r_a$, equation (22) can be written as

$$V_\theta = \frac{Br_j^3}{6} \tan^3 r_a. \tag{24}$$

It can be derived from this that

$$V_B = \frac{Br_j^3}{6}\left(\tan^3\theta_{21} + \tan^3\theta_{22} + \tan^3\theta_2 - \tan^3\theta_{11} - \tan^3\theta_{12} - \tan^3\theta_1\right). \tag{25}$$

θ_1, θ_{11}, θ_{12}, θ_2, θ_{21}, and θ_{22} are the spread angles corresponding to the meshing points.

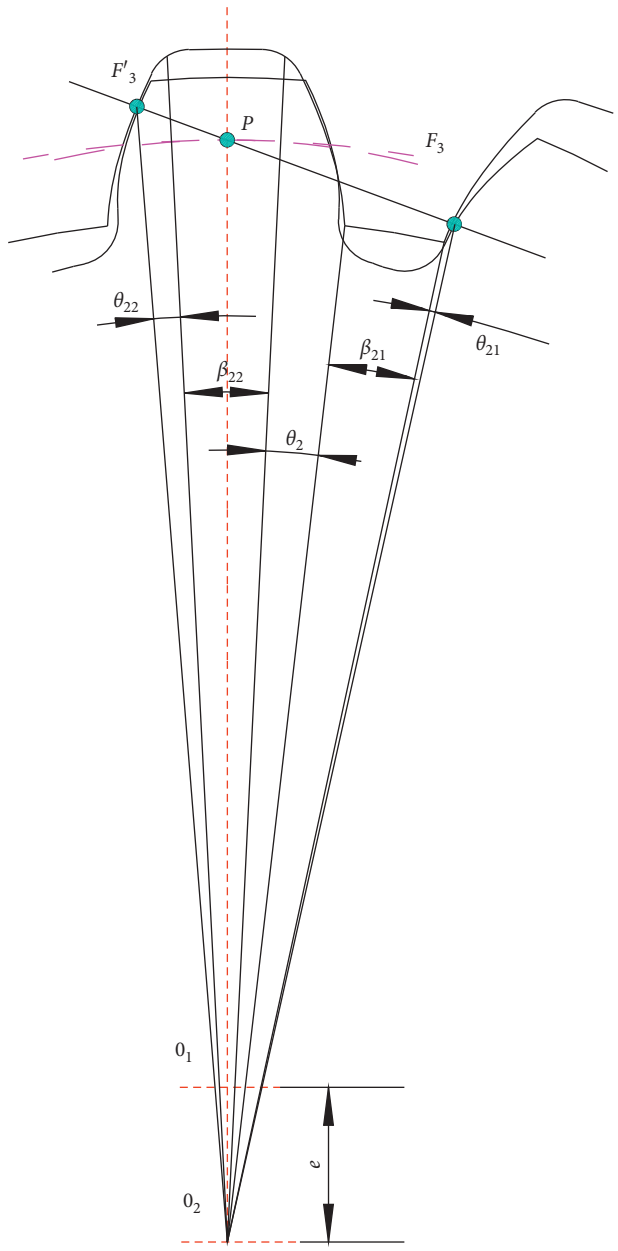

Figure 5: The relationship between the trapped oil and the rotation angle of the internal gear.

According to equations (15) and (19), (20), and (25), V_0 can be obtained.

From equation (16) and (17), the positions of V_{10} and V_{20} are shown in Figures 7 and 8, respectively. V_{10} and V_{20} can be obtained from (19), (20), (24), and (25).

2.4. Unloading Area. As shown in Figure 9, points P, F are node and meshing points, respectively. Let the length of P, F be f, and the relationship between f and the gear rotation angle φ is [18]

$$f(\varphi) = 0.5t_j - r_j\left(\varphi - \frac{\pi}{z}\right). \tag{26}$$

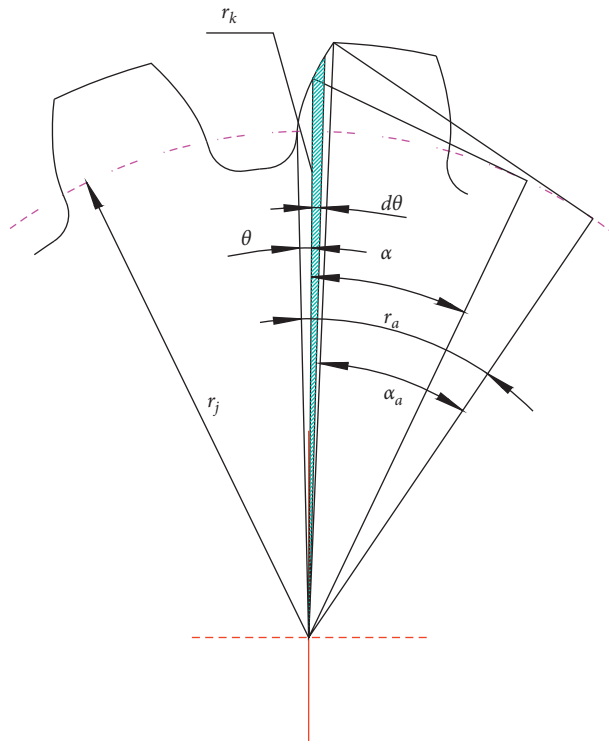

Figure 6: The relationship between area and expansion angle.

The unloading area is the area where the cross section of the trapped oil volume is located in the unloading groove [19]. In Figure 9, the calculation steps of S_{u1v1} and S_{u2v2} are as follows: (1) Calculate the expression of $f(\varphi)$ at points F, 1, 2, 3, 4, 5, 6 on the gear tooth profile. (2) Find the curve equations of 12, 23, 34, 4F, F5, 56. (3) Solve the integral to calculate the unloading area, the method, and steps referring to [20].

In the calculation process of S_{u2v2}, $f(\varphi)$ can be replaced with $[t_j - f(\varphi)]$, and the other steps can be calculated according to S_{u1v1}.

V_a, V_b are the actual trapped oil volume:

$$\begin{aligned} V_a &= V_1 - S_{u1v1}, \\ V_b &= V_2 - S_{u2v2}. \end{aligned} \tag{27}$$

3. Oil Trapped Pressure Model of Internal Gear Pump

Figure 10 shows the trapped oil pressure model of the internal gear pump. Let the pressures of V_1, V_2, inlet chamber, and outlet chamber be P_1, P_2, P_{in}, and P_{out}, respectively. Let q_1, q_2, and q_h be the unloading flow rate from the trapped oil cavity V_1 to the oil outlet cavity, the unloading flow rate from the trapped oil cavity V_2 to the oil inlet cavity, and the unloading flow rate from the trapped oil cavity V_2 to trapped oil cavity V_1, respectively. According to fluid mechanics and dynamics, the following is derived:

$$\begin{cases} q_1 = CV_a\sqrt{\dfrac{2}{\rho}}\sqrt{\left|P_1 - P_{\text{out}}\right|}\,\text{sign}\left(P_1 - P_{\text{out}}\right), \\ q_2 = CV_b\sqrt{\dfrac{2}{\rho}}\sqrt{\left|P_2 - P_{\text{in}}\right|}\,\text{sign}\left(P_2 - P_{\text{in}}\right), \\ q_h = CV_h\sqrt{\dfrac{2}{\rho}}\sqrt{\left|P_1 - P_2\right|}\,\text{sign}\left(P_1 - P_2\right), \end{cases}$$

$$\begin{cases} q_1 + q_h = -\dfrac{\mathrm{d}V_a}{\mathrm{d}t} - \dfrac{V_a}{\beta}\dfrac{\mathrm{d}P_1}{\mathrm{d}t}, \\ q_2 - q_h = -\dfrac{\mathrm{d}V_b}{\mathrm{d}t} - \dfrac{V_b}{\beta}\dfrac{\mathrm{d}P_2}{\mathrm{d}t}, \end{cases} \tag{28}$$

$$\begin{cases} \dfrac{\mathrm{d}P_1}{\mathrm{d}t} = -\dfrac{\beta}{V_a}\left[(q_1 + q_h) + \dfrac{\mathrm{d}V_a}{\mathrm{d}t}\right], \\ \dfrac{\mathrm{d}P_2}{\mathrm{d}t} = -\dfrac{\beta}{V_b}\left[(q_2 - q_h) + \dfrac{\mathrm{d}V_b}{\mathrm{d}t}\right]. \end{cases}$$

In above equations, ρ, β are the density and bulk elastic modulus of the fluid, respectively. C is the flow coefficient 0.60–0.65. $V_h = h_j \times B$.

According to $\mathrm{d}\varphi = \omega \mathrm{d}t$,

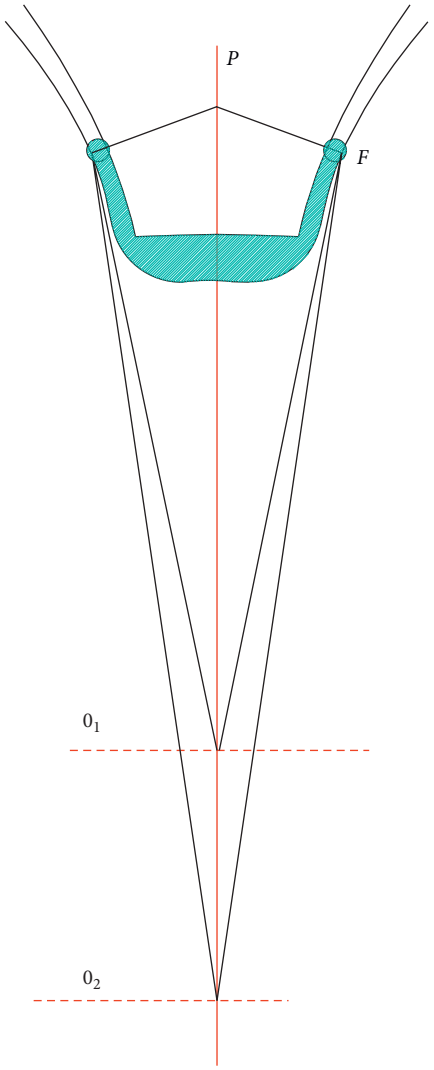

Figure 7: The Minimum value of V_{10}.

$$\begin{cases} \dfrac{dP_1}{d\varphi} = -\dfrac{\beta}{\omega V_a}\left[(q_1 + q_h) + \omega\dfrac{dV_a}{d\varphi}\right], \\ \dfrac{dP_2}{d\varphi} = -\dfrac{\beta}{\omega V_b}\left[(q_2 - q_h) + \omega\dfrac{dV_b}{d\varphi}\right]. \end{cases} \tag{29}$$

Let, $k_1 = (\beta/\omega)C\sqrt{2/\rho}$, $k_2 = (2\pi/z)Br_j^2$, $k_3 = (2\pi/z)(1 - (2h_j/t_j))\ Br_j^2$, $k_4 = (\pi/2z)(1 - (2h_j/t_j))$, $k_5 = (3\pi/2z)$, $k_6 = \beta k_2$, $k_7 = \beta k_3$, $k_8 = V_h k_1$.

Then,

$$\begin{cases} \dfrac{dP_1}{d\varphi} = -k_1\sqrt{P_1 - P_{out}} - \dfrac{k_8\sqrt{P_1 - P_2}}{V_{10} + 0.5k_3[\varphi - k_4]^2} - \dfrac{k_7[\varphi - k_4]}{V_{10} + 0.5k_3[\varphi - k_4]^2}, \\ \dfrac{dP_2}{d\varphi} = -k_1\sqrt{P_2 - P_{in}} + \dfrac{k_8}{V_{20} + 0.5k_2(\varphi - k_5)^2}\sqrt{P_1 - P_2} - \dfrac{k_6(\varphi - k_5)}{V_{20} + 0.5k_2(\varphi - k_5)^2}. \end{cases} \tag{30}$$

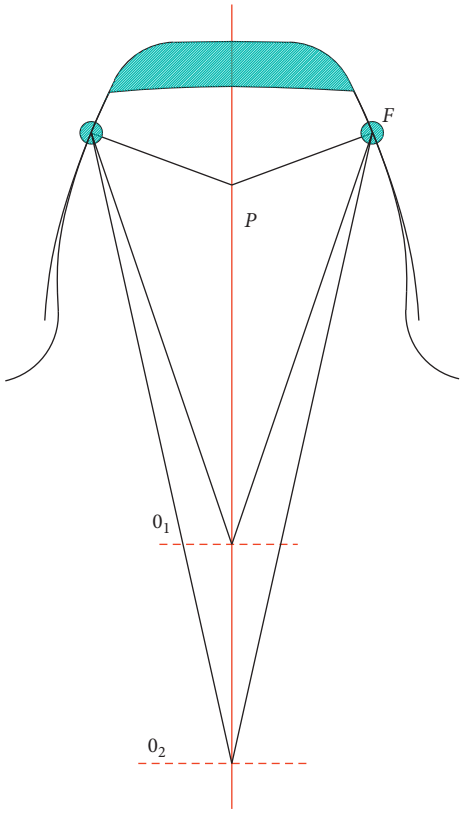

Figure 8: The Minimum value of V_{20}.

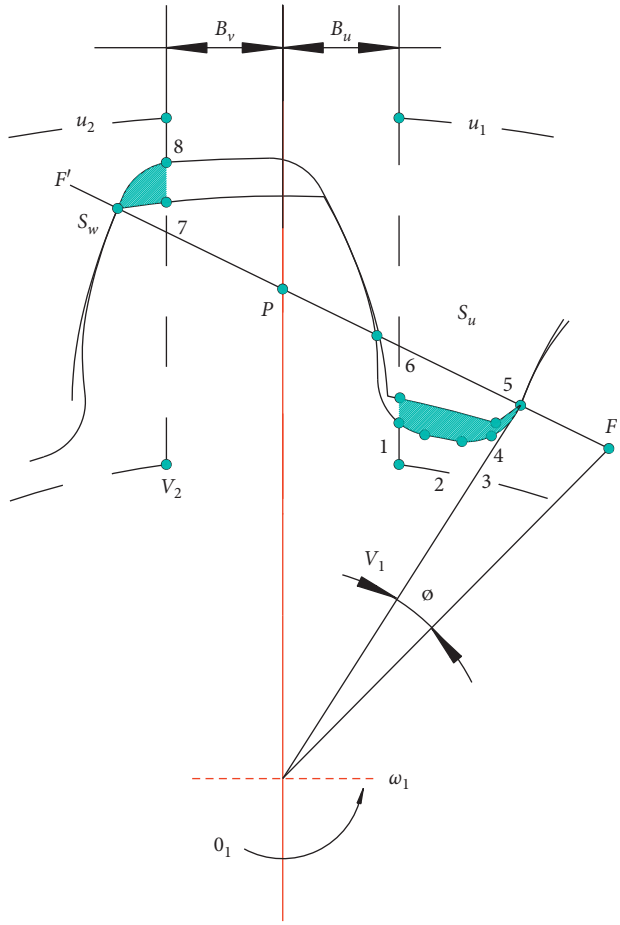

Figure 9: Calculation of the unloading area.

4. Simulation Research

4.1. Gear Parameters and Simulation. Input parameters, modulus $m = 3$, pressure angle $\alpha = 20°$, tooth number $z_1/z_2 = 13/19$, addendum height coefficient $h_{a1}/h_{a2} = 1/1$, radial clearance coefficient $c_{n1}/c_{n2} = 0.25/0.25$, total tooth height $h_{f1}/h_{f2} = 6.734/6.766$, tool fillet $r_0 = 0.25$, the profile shift coefficient $x_1/x_2 = 0.432/0.504$, and base pitch $t_j = 8.856$. According to MATLAB simulation by equations (4) and (5), a pair of gears processed by the generative method is shown in Figure 11.

4.2. Simulation Results. When the inlet pressure $p_i = 0$ MPa and the outlet pressure $p_o = 10$ MPa , the rotation process of the gear pair is simulated. During this process, the change trend of the trapped oil volumes V_1, V_2, V is shown in Figure 12. It can be seen that the change of V_1, V_2 is parabolic. When the rotation angle is 0.12 rad, the minimum value is 2.34 mm^3, and when the rotation angle is 0.36 rad, the minimum value is 2.12 mm^3. V is the sum of V_1 and V_2, and its changing trend is to first reach a low point and then present an increasing trend. Internal gear pumps and external gear pumps have similar changes [21, 22]. During a period of gear tooth meshing, simulate the pressure changes in V_1 and V_2. There is no backlash between the front gear and the rear gear. When $h_j = 0$, the changes of p_1 and p_2 are shown in Figure 13. p_1 and p_2 have a large variation range, and there are positive pressure and negative pressure in the interval. When the gear rotation angle reaches 0.12 rad, p_1 reaches the peak value of 35.5 MPa. When the corner reaches 0.36 rad, p_2 reaches the peak value of 40.2 MPa. If there is a backlash between the front gear and the rear gear, when $h_j = 0.06$ m, the changes of p_1 and p_2 are shown in Figure 14. It can be seen that the pressure change trend in the trapped oil zone is similar to that in Figure 13, but the change range is convergent. When the turning angle reaches 0.12 rad, p_1 reaches the peak value of 30.2 MPa. When the rotation angle reaches 0.36 rad, p_2 reaches the peak value of 20.24 MPa. If there is tooth side clearance $h_j = 0.06$ m, and a rectangular unloading groove is designed in the oil trapped area, the position of the boundary line of the unloading groove is $B_v = B_u = 0.5\pi m$, and the pressure change trend in the oil trapped area is shown in Figure 15. The change trends of p_1 and p_2 are very similar to those in Figures 13 and 14, and the range of change is more convergent. When the rotation angle reaches 0.12 rad, p_1 reaches the peak value of 16.5 MPa, and when the rotation angle reaches 0.36 rad, p_2 reaches the peak value of 18.2 MPa. Internal gear pumps have lower trapped oil pressure than external gear pumps [23] and arc gear pumps [24]. The design of tooth side clearance and unloading groove can slow down trapped oil pressure and reduce peak pressure.

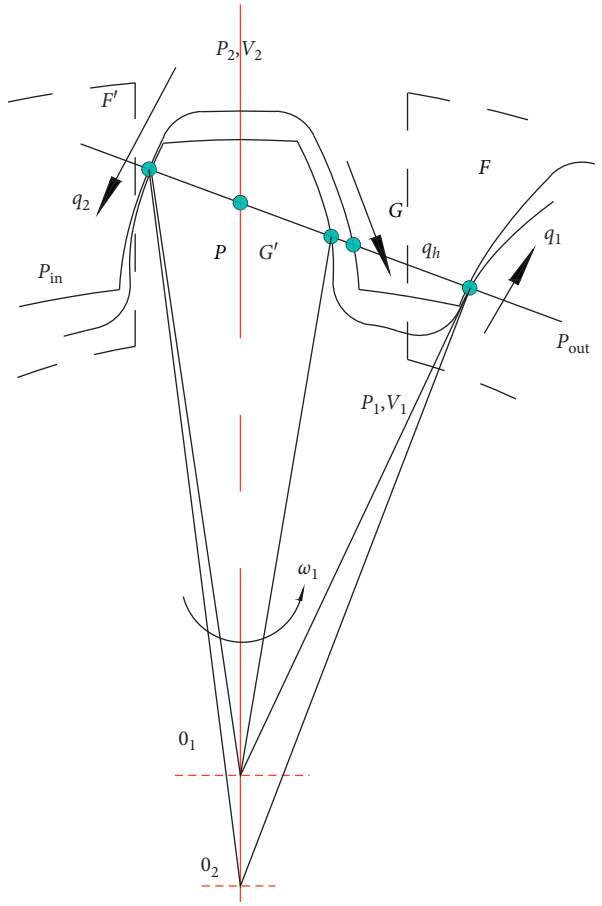

Figure 10: Trapped oil pressure model of the internal gear pump.

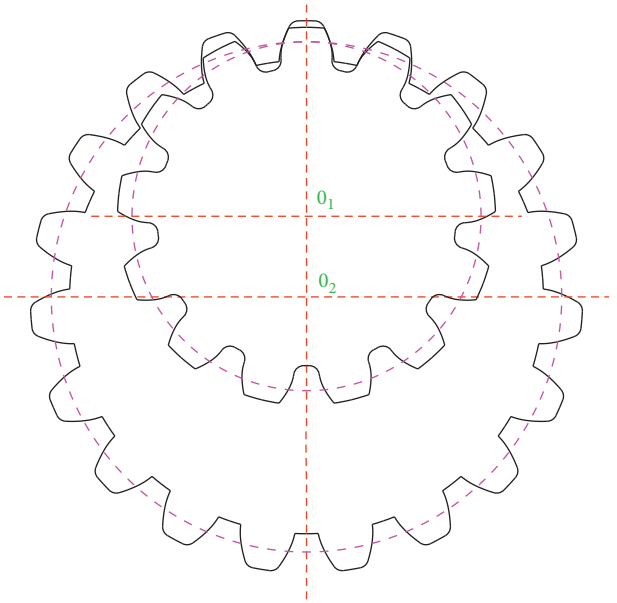

Figure 11: A pair of gears processed by the generative method.

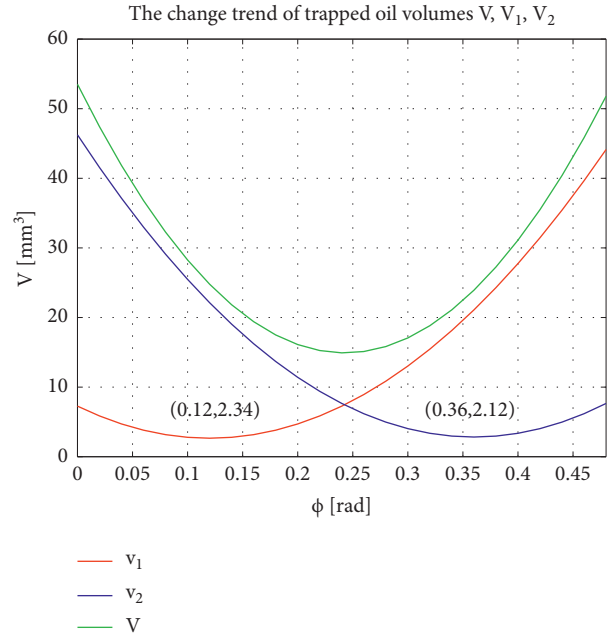

Figure 12: Changes in trapped oil volume.

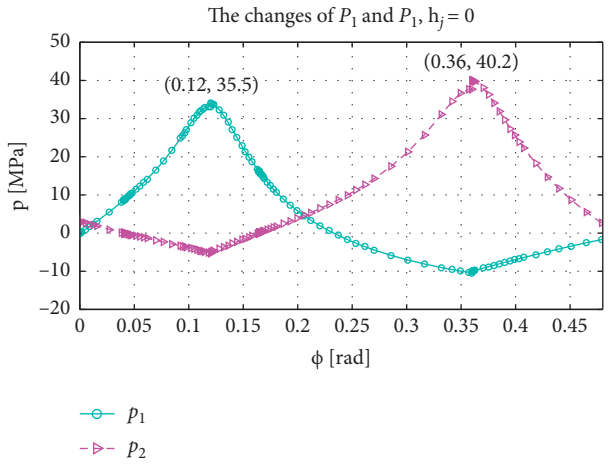

Figure 13: $h_j = 0$, changes in trapped oil pressure.

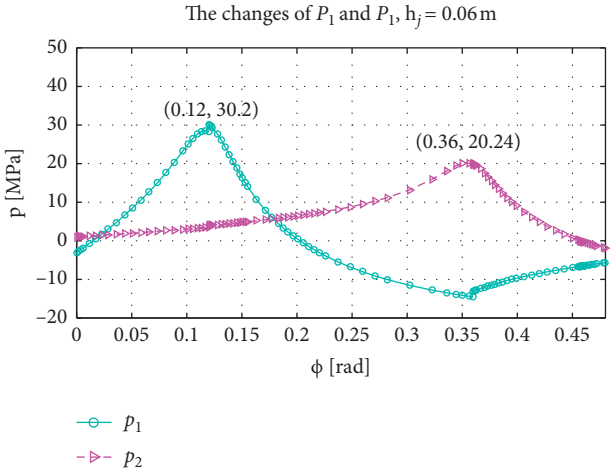

Figure 14: $h_j = 0.06$ m, changes in trapped oil pressure.

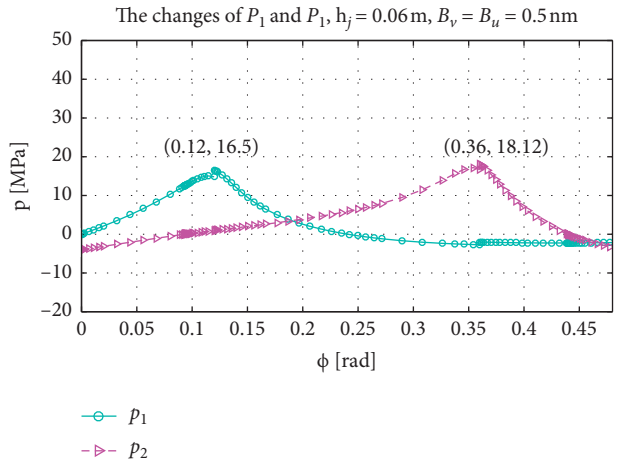

FIGURE 15: $h_j = 0.06$ m, $B_v = B_u = 0.5\pi m$, changes in trapped oil pressure.

5. Conclusions

(1) For a pair of internal gear pairs processed by the generative method, there are oil trapped areas between the gear teeth during meshing, and the trapped oil volumes V_1 and V_2 present a parabolic change law, and each has a minimum value, which changes periodically when the gear rotates.

(2) When the internal gear pump rotates, the trapped oil pressures p_1 and p_2 increase first and then decrease with the change of the rotation angle. There is a maximum peak value. When the volume of the trapped oil cavity is the smallest, the trapped oil pressure reaches the maximum.

(3) The tooth side clearance will improve the oil trapping characteristics of the internal gear pump and reduce the pressure peak in the trapped oil cavity.

(4) The design of the unloading groove will improve the fluidity of trapped oil, reduce the range of trapped oil pressure, and reduce the pressure peak in the trapped oil cavity.

Nomenclature

AB: The outer contour of the rack cutter
BC: The outer contour of the rack cutter
CD: The outer contour of the rack cutter
DE: The outer contour of the rack cutter
h_a: Addendum height
h_{a1}: Addendum height
h_{a2}: Addendum height
c_n: Head clearance coefficient
h_f: Total tooth height
h_{f1}: Total tooth height
h_{f2}: Total tooth height
r_0: Tool fillet
α: Pressure angle
x: The profile shift coefficient
x_1: The profile shift coefficient
x_2: The profile shift coefficient
p: Pitch
$s_t(O_t x_t y_t)$: A rectangular coordinate system
O_s: Center of gear O_s
$O_{s'}$: Center of gear $O_{s'}$
$s_s(O_s x_s y_s)$: A rectangular coordinate system of gear O_s
$s_{s'}(O_{s'} x_{s'} y_{s'})$: A rectangular coordinate system of gear $O_{s'}$
$s_e(O_e x_e y_e)$: A rectangular coordinate system
x_t: Displacement direction
s: Displacement
O_e: Origin of s_e
φ_s: The rotation angle
r_s: The gear pitch radius
m: The modulus of the gear
z: The number of teeth
z_1: The number of teeth
z_2: The number of teeth
$R_s^p(\varphi_s, x_t)$: The envelope of the tooth profile surface family of the rack tool
$M_{st}(\varphi_s)$: The transformation matrix
s_s: The coordinate system
s_t: The coordinate system
$R_t^p(\varphi_{s'}, x_t)$: The envelope of the rack tool tooth profile surface family
$M_{s't}(\varphi_{s'})$: The transformation matrix
$s_{s'}$: The coordinate system
Q_{sh}: The theoretical instantaneous flow
B: The gear face width
ω: The angular velocity of the gear pump
r_a: The addendum circle radius
r: The gear reference radius
r_j: The gear base circle radius
φ: The driving gear rotation angle
V_{sh}: The scanning volume
φ_F: The rotation angle of F
φ_G: The rotation angle of G
$\varphi_{G'}$: The rotation angle of G'
$\varphi_{F'}$: The rotation angle of F'
h_j: The length between G and G'
t_j: The base pitch
V: Trapped oil volume
V_1: Trapped oil volume
V_2: Trapped oil volume
V_0: The minimum values of V
V_{10}: The minimum values of V_1
V_{20}: The minimum values of V_2
$V^{\frown}$: O_1, F, F', sector area
$V^{\overset{\frown}{o1F'F}}$: O_2, F, F', sector area
$V^{\overset{\frown}{o2F'F}}$: O_2, G', F_3, sector area
$V_{\Delta o1o2F}^{o1G'F3}$: O_1, O_2, F, triangle area
$V_{\Delta o1o2F'}$: O_1, O_2, F', triangle area
e: The distance between the centers of the gear
α': The meshing angle of the gear pair
V_A: The unchanged area
V_B: The changing area
$r_{a,1}$: The addendum circle
$r_{a,2}$: The addendum circle
β_{12}: Addendum angle

β_{21}: Addendum angle
$r_{f,2}$: The tooth root circle
$r_{f,1}$: The tooth root circle
β_{11}: Tooth root circle included angle
β_{21}: Tooth root circle included angle
θ: The spread angle
r_k: The radius on the tooth profile
θ_1: The spread angles corresponding to the meshing points
θ_{11}: The spread angles corresponding to the meshing points
θ_{12}: The spread angles corresponding to the meshing points
θ_2: The spread angles corresponding to the meshing points
θ_{21}: The spread angles corresponding to the meshing points
θ_{22}: The spread angles corresponding to the meshing points
P: Node
F: Meshing point
f: The length of$P$, F
S_{u1v1}: The unloading area
S_{u2v2}: The unloading area
$f(\varphi)$: The relationship between f and the gear rotation angle φ
P_1: The pressures of V_1
P_2: The pressures of V_2
P_{in}: The pressures of the inlet chamber
P_{out}: The pressures of the outlet chamber
q_1: The unloading flow rate from the trapped oil cavity V_1 to the oil outlet cavity
q_2: The unloading flow rate from the trapped oil cavity V_2 to the oil inlet cavity
q_h: The unloading flow rate from the trapped oil cavity V_2 to trapped oil cavity V_1
ρ: The density
β: Bulk elastic modulus of the fluid
C: The flow coefficient
V_h: Tooth side clearance volume
c_{n1}: Radial clearance coefficient
c_{n2}: Radial clearance coefficient.

Data Availability

The data used to support the findings of this study are available from the corresponding author upon request.

Conflicts of Interest

The authors declare that there are no conflicts of interest regarding the publication of this paper.

Acknowledgments

This work was supported by Fujian Jiangxia College Cultivation Project (JXZ2019015), the Natural Science Foundation of Fujian Province (2020J01932), and Program for New Century Excellent Talents in Fujian Province University (Minjiaoke[2018] no. 47).

References

[1] X. Hao, X. Zhou, X. Liu, and X. Sang, "Pressure ripple of gear pumps affected by air content on trapped volume," *Journal of Vibroengineering*, vol. 18, no. 6, pp. 4033–4041, 2016.
[2] P. Antoniak, J. Stryczek, M. Banaś et al., "Visualization research on the influence of an ultrasonic degassing system on the operation of a hydraulic gear pump," *MATEC Web of Conferences*, vol. 211, p. 03005, 2018.
[3] H. Tian, "Dynamic pressure simulation of an external gear pump with relief chamber using a morphological approach," *IEEE Access*, vol. 6, pp. 77509–77518, 2018.
[4] P. Antoniak and J. Stryczek, "Visualization study of the flow processes and phenomena in the external gear pump," *Archives of Civil and Mechanical Engineering*, vol. 18, no. 4, pp. 1103–1115, 2018.
[5] F. Sun, Y. Li, C. Wen, and F. Zhong, "Demarcated standard and verification of backlash relief in external gear pumps," *Nongye Gongcheng Xuebao/Transactions of the Chinese Society of Agricultural Engineering*, vol. 33, no. 20, pp. 61–66, 2017.
[6] M. Hao, Y. Zhou, and S. Hao, "Manufacturing and study on influence of changes in center distance in circle arc-involute-circle arc gear pump operating at high pressure and high speed," *Proceedings of the Institution of Mechanical Engineers, Part C: Journal of Mechanical Engineering Science*, vol. 230, no. 18, pp. 3285–3297, 2016.
[7] H. Zhou, R. Du, A. Xie, and H. Yang, "Investigations of the micro surface shape for the gear-shaft/journal-bearing interface in water hydraulic internal gear pumps," *Advances in Mechanical Engineering*, vol. 9, no. 11, pp. 1–15, 2017.
[8] Y. Sun, Y. Yu, and Z. Qi, "Optimization of PGH type gear pump vibration and noise reduction," *Journal of Liaoning Technical University (Natural Science Edition)*, vol. 37, no. 4, pp. 746–749, 2018.
[9] M. Rundo, "Models for flow rate simulation in gear pumps: a review," *Energies*, vol. 10, no. 9, p. 1261, 2017.
[10] G. Li, L. Zhang, and W. Han, "Profile design and displacement analysis of the low pulsating gear pump," *Advances in Mechanical Engineering*, vol. 10, no. 3, pp. 179–189, 2018.
[11] J. Zhang and S. Li, "3D flow field analysis of multi-gear pump," *Liaoning Gongcheng Jishu Daxue Xuebao (Ziran Kexue Ban)/Journal of Liaoning Technical University (Natural Science Edition)*, vol. 35, no. 7, pp. 765–769, 2016.
[12] V. N. Syzrantsev and A. A. Pazyak, "Precessional gears for drives of stop valves of oil and gas pipelines and gearboxes of pumps to produce heavy crude oil," *Bulletin of the TOMSK Polytechnic University-Geo Assets Engineering*, vol. 328, no. 2, pp. 15–27, 2017.
[13] M. Rundo, "Theoretical flow rate in crescent pumps," *Simulation Modelling Practice and Theory*, vol. 71, pp. 1–14, 2017.
[14] Z. Chen, R. Xu, L. He, and J. Liao, "Modeling an internal gear pump," in *Proceedings of the AIP Conference, 1967*, no. 1, Article ID 040049, Busan, South Korea, 1967.
[15] K. Park, M. Chang, and D. Jeon, "Precise flowrate control of fluid gear pumps in automated painting systems using a repetitive controller," *Applied Sciences*, vol. 9, no. 16, p. 3413, 2019.
[16] J. Mo, X. Pan, C. Gu, S. Zheng, and G. Ying, "A thermo-hydrodynamic analysis of the self-lubricating bearings applied in gear pumps using computational fluid dynamics method," *Journal of Tribology*, vol. 140, no. 1, 9 pages, 2018.

[17] G. Li, L. Zhang, W. Han, X. Deng, and Y. Feng, "Pulsation characteristic analysis and tooth profile design of double-circular-arc helical gear pumps," *China Mechanical Engineering*, vol. 29, no. 2, pp. 186–192, 2018.

[18] Y. Li, "Impact analysis of composite stiffness in gear pair of external gear pump," *Transactions of the Chinese Society of Agricultural Engineering*, vol. 27, no. 4, pp. 153–157, 2011.

[19] Y. Li, K. Liu, and F. Sun, "Dynamic model of gears with trapped oil and coupled analysis in external spur-gear pump," *Mechanical And Electronics Engineering III*, vol. 130-134, pp. 610–615, 2011.

[20] S. Guo and D. Chen, "Calculation of unloading area of internal gear pump and optimization," *Mathematical Problems in Engineering*, vol. 2020, Article ID 7319871, 9 pages, 2020.

[21] X. Zhao and A. Vacca, "Numerical analysis of theoretical flow in external gear machines," *Mechanism and Machine Theory*, vol. 108, pp. 41–56, 2017.

[22] Y. Li and F. Sun, "Simulation and theoretical analysis on trapped oil pressure in external gear pump influenced by vibration," *Transactions of the Chinese Society of Agricultural Engineering*, vol. 28, no. 13, pp. 77–81, 2012.

[23] E. Frosina, A. Senatore, and M. Rigosi, "Study of a high-pressure external gear pump with a computational fluid dynamic modeling approach," *Energies*, vol. 10, no. 6, p. 1113, 2017.

[24] X. Wu, C. Liu, W. Gan, X. Wang, S. Hu, and J. Ji, "Robust design of external gear pump with trapped oil problem," *Hangkong Dongli Xuebao/Journal of Aerospace Power*, vol. 30, no. 11, pp. 2721–2729, 2015.